Nanofluidic Osmotic Diodes: Theory and Molecular Dynamics Simulations

Clara B. Picallo,[1] Simon Gravelle,[1] Laurent Joly,[1,*] Elisabeth Charlaix,[2] and Lydéric Bocquet[1,3,†]

[1]*Institut Lumière Matière, UMR5306 Université Lyon 1-CNRS, Université de Lyon 69622 Villeurbanne, France*
[2]*Laboratoire interdisciplinaire de Physique, UMR5588 Université Joseph Fourier-CNRS 38402 Grenoble, France*
[3]*Department of Civil and Environmental Engineering, Massachusetts Institute of Technology, Cambridge, Massachusetts 02139-4307, USA*

(Received 8 May 2013; published 11 December 2013)

Osmosis describes the flow of water across semipermeable membranes powered by the chemical free energy extracted from salinity gradients. While osmosis can be expressed in simple terms via the van 't Hoff ideal gas formula for the osmotic pressure, it is a complex phenomenon taking its roots in the subtle interactions occurring at the scale of the membrane nanopores. Here we use new opportunities offered by nanofluidic systems to create an osmotic diode exhibiting asymmetric water flow under reversal of osmotic driving. We show that a surface charge asymmetry built on a nanochannel surface leads to nonlinear couplings between water flow and the ion dynamics, which are capable of water flow rectification. This phenomenon opens new opportunities for water purification and complex flow control in nanochannels.

DOI: 10.1103/PhysRevLett.111.244501 PACS numbers: 47.61.Fg, 47.11.Mn, 47.85.L−, 82.39.Wj

A number of new nanofluidic devices with striking electric and hydrodynamic properties have been developed in recent years, benefiting from the predominance of surface effects over bulk ones at the nanoscale [1]. In particular, the dimensions of nanofluidic systems are usually comparable to the size of the electrical double layer (EDL), the distance over which significant charge separation occurs in the vicinity of the channel walls. The overlap of the EDLs induces strong electrostatic interactions in the nanochannel, which markedly modify the ion dynamics and lead to a number of new functionalities [2]. One of the most appealing applications is the nanofluidic ionic diode mimicking the behavior of a semiconductor diode, here for ion transport. This simple integrable device is able to induce electric current rectification [3,4] by tuning the channel geometry [5,6] or the surface charge [7,8]. While such devices have brought the possibility to control electric current in an efficient manner, it is now highly desirable to propose alternative mechanisms to control fluid flow at the nanoscale. To achieve that aim, a powerful driving force is the osmotic pressure $\Delta\Pi$, as given by the van 't Hoff formula

$$\Delta\Pi = k_B T \Delta n_{\mathrm{sol}}, \tag{1}$$

with Δn_{sol} the solute concentration difference across a semipermeable membrane [9]. Osmosis is a fundamental transport process for water in all living systems, and its applications are numerous, in particular, for water desalination and energy harvesting [10–12]. It has motivated many works in the last few years in order to explore its molecular mechanisms at the nanoscale [13–16].

Here we explore the possibility of creating an osmotic diode and osmotic flow rectification. Rectified osmosis with asymmetric water permeability under solute gradient reversal was actually reported in a number of biological cell systems, such as erythrocytes [17], granulocytes [18], epithelial cells [19], or COS-7 fibroblasts [20]. The origin of this osmotic rectification remains, however, not understood up to now. We show that a similar functionality can be obtained on the basis of nonlinear flow-ion couplings in nanochannels, with an asymmetric surface charge along the channel surface.

Osmosis and osmotic diode.—We start by exploring the osmotic response of a charged nanochannel subject to a salinity gradient, and first identify the mechanisms at the very origin of osmotic pressure. Let us consider a nanochannel of length L and height h. Each end of the channel is in contact with a salt reservoir of concentration $n_L = n_0 - \Delta n/2$ and $n_R = n_0 + \Delta n/2$ in the left and right ends, respectively. An additional voltage drop $\Delta V = V_R - V_L$ between the ends of the channel will be also considered. Our final aim is to consider asymmetric channels, as sketched in Fig. 1. However, the following discussion on the origin of osmotic pressure applies very generally to any charged nanochannel. To ensure electroneutrality, EDLs build up at the charged surfaces that may overlap depending on the height of the channel and salt concentration.

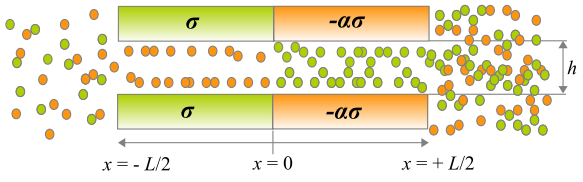

FIG. 1 (color online). Sketch of the system showing the asymmetry of surface charge in the nanochannel, and the different salt concentrations in the left and right reservoirs.

Dynamic origin of the osmotic pressure.—In the classical osmosis configuration, i.e., if the nanochannel behaves as a semipermeable membrane to ions, an osmotic pressure drop $\Delta\Pi$ builds up and induces a water flow toward the reservoir with the largest salt concentration. However, in full generality the nanochannel is usually only partially semipermeable, meaning that ions may still permeate through it, although this process is strongly affected by the surface charge [2]. Building on the seminal works by Kedem and Katchalsky [9] and Manning [21], we show in the following that an osmotic pressure still applies on the solvent and that it can be derived from a simple force balance in the nanochannel.

Let us focus on water dynamics inside the nanochannel: the force balance on water takes the form of the Stokes equation for the velocity field v and the hydrodynamic pressure P, with a supplementary electric force $n_c(-\nabla V)$ due to local charge imbalance:

$$\eta\nabla^2 v - \nabla P + n_c(-\nabla V) = 0, \tag{2}$$

where $n_c = e(n_+ - n_-)$ is the local charge density ($n_\pm$ the densities of cations and anions assumed monovalent to simplify), e the elementary charge, η the fluid viscosity, and V the local electric potential. Integrated over the nanochannel, this allows us to express the total water flux Q as

$$Q = \mathcal{A}\,\mathcal{L}_{\rm hyd}\frac{-\Delta[P - \Pi_{\rm app}]}{L}, \tag{3}$$

with $\mathcal{L}_{\rm hyd}$ the hydrodynamic permeability of the channel and $\Delta\Pi_{\rm app}$ the total electric driving force per channel cross section $\mathcal{A}$ defined as

$$\Delta\Pi_{\rm app} = \frac{1}{\mathcal{A}}\int d\mathcal{A}\int_0^L dx\, n_c(-\nabla V). \tag{4}$$

Combined with Eq. (3), this allows us to interpret the electric force acting along the channel, $\Delta\Pi_{\rm app}$, as an apparent osmotic pressure. In the absence of steric exclusion of the ions in the permeable pore as considered here, only this contribution to the osmotic pressure exists so that $\Delta\Pi_{\rm app}$ identifies with the full osmotic pressure.

A general relationship is now obtained connecting $\Delta\Pi_{\rm app}$ to the ion fluxes $J_\pm$ through the nanochannel. To that aim, we assume that the ion dynamics obeys the Poisson-Nernst-Planck (PNP) transport equations [1], thus, assuming a 1D geometry with the various quantities averaged over the cross area, depending only on the x coordinate along the channel [22]. The PNP framework introduces the ion fluxes as a key quantity defined as $J_\pm = -D\nabla n_\pm \mp \mu n_\pm e\nabla V$, with D the ion diffusion coefficient and $\mu = D/k_BT$ the mobility taken to be the same for both species. Note that we neglected the advection contribution to the fluxes. For the low velocities expected in nanometric channels, the corresponding Peclet number $\mathrm{Pe} = vL/D$ (v the velocity, L the channel length, and D the ion diffusion coefficient) is expected to remain small, although some Peclet of order 1 may be reached. This is in any case a first approximation of the full dynamics, which allows us to discuss the main physical mechanisms at work. The effect of advection can be subsequently introduced as corrections to the present contributions, as done, e.g., in Ref. [21] for neutral solutes. In the stationary state, the ion fluxes are homogeneous in space and time, leading to spatially constant electric flux $J_e = e(J_+ - J_-)$ and solute flux $J_s = J_+ + J_- = -D\nabla n_{\rm sol} - \mu n_c\nabla V$, with $n_{\rm sol} = n_+ + n_-$ the total ion concentration. Using this relation to express the electric force $n_c(-\nabla V)$ as a function of the solute flux J_s, Eq. (4), thus, can be rewritten as

$$\Delta\Pi_{\rm app} = k_BT\left(\Delta n_{\rm sol} + J_s \times \frac{L}{D}\right), \tag{5}$$

where $\Delta n_{\rm sol} = 2\Delta n$ and $\Delta n = n_R - n_L$ the salt concentration difference (the factor of 2 coming from the two ion species). Note that an equivalent relation was obtained by Manning [21] using a generic potential-energy profile to represent the membrane. In the absence of solute flux $J_s = 0$, the previous equation reduces to $\Delta\Pi_{\rm app} = k_BT\Delta n_{\rm sol}$; i.e., it matches the van 't Hoff expression for the osmotic pressure drop across a perfectly semipermeable membrane. For a fully permeable neutral channel, $J_s = -D\Delta n_{\rm sol}/L$ and $\Delta\Pi_{\rm app} = 0$, as also expected. In general, the nanochannel is only partly permselective, and $\Delta\Pi_{\rm app}$ takes a nonvanishing value depending on the solute flux. Altogether, the driving force acting on the water, thus, takes the value $\Delta P_{\rm TOT} = \Delta P - \Delta\Pi_{\rm app}$, and $\Delta\Pi_{\rm app}$ is the apparent osmotic pressure that one needs to overcome in order to counteract osmosis.

Towards the osmotic diode.—We are now in position to obtain an analytical expression for the apparent osmotic pressure based on Eq. (5). In the following, we will discuss more specifically a geometry with an asymmetric surface charge as sketched in Fig. 1: the left side has a positive surface charge density σ while the right side has a negative surface charge $-\alpha\sigma$, with $\alpha > 0$ a numerical coefficient. In a similar geometry for the ionic diode, it has been shown that the corresponding 1D PNP equations obeyed by the ion concentrations can be solved for an applied voltage drop ΔV across the nanochannel [8,23,24].

In contrast, no solution exists up to now for the response under osmotic gradients Δn. This is our purpose here to derive such a solution. Our derivation follows the general strategy of previous works [8,23,24]. First, it should be noted that the surface charge carried by the walls leads to a local ion charge imbalance inside the nanochannel, $n_+ - n_- = -2\Sigma/h$, with $\Sigma = \sigma/e > 0$ and $\Sigma = -\alpha\sigma/e$ for the left and right parts, respectively, Fig. 1. Accordingly, at equilibrium (i.e., $n_R = n_L = n_0$), a Donnan potential V_D builds up in the nanochannel in order to ensure a spatially homogeneous electrochemical potential over the system [1], $\mu_\pm = k_BT\log(n_\pm) \pm eV_D \equiv \mu_0 = k_BT\log(n_0)$. Together with the charge electroneutrality condition, this

provides expressions for the local ion concentrations and Donnan potential V_D in the nanochannel. Now, under the combined action of a voltage drop ΔV and an osmotic forcing Δn, nonequilibrium ion fluxes $J_\pm$ build up in the system. Using the spatial homogeneity of the fluxes along the nanochannel in the stationary state, with $J_\pm = -D\nabla n_\pm \mp \mu n_\pm e\nabla V$ at the level of PNP equations, one may deduce the spatial dependence of ion densities and potential. We report the detailed (cumbersome) calculations in the Supplemental Material [25]. Now, one should treat specifically the discontinuities associated with the step change of the surface charge from the two reservoirs to the inner nanochannel ends, as well as at the junction between the two sides of the nanochannel with different surface charge. Following previous descriptions [8,23,24], which made use of the analogy of the problem with p-n junctions in semiconductors, one may treat these discontinuities by neglecting the extension of the space charge zone and writing accordingly the continuity of the electrochemical potential. Neglecting the subtle effects at junctions and channel ends constitutes obviously a simplifying assumption, which allows us to obtain an analytical prediction for the transport properties and osmotic pressure. However, such assumptions were shown to provide *in fine* a good description of transport comparing favorably with experiments and numerical calculations [8,24].

As demonstrated in the Supplemental Material [25], an analytical solution of the PNP equations with these junction conditions can then be found in the regime of high surface charge. This is quantified by a large dimensionless number $\delta = |\Sigma|/hn_0$ defined as the surface-to-bulk-charge ratio [26]. This dimensionless number compares the number concentration of surface charge carriers ($\sim|\Sigma|/h$) to its bulk counterpart ($\sim n_0$) [1]. Altogether, in the regime $\delta \gg 1$, one obtains analytical expressions for the concentrations profiles and electrostatic potential, as well as for corresponding solute and electric fluxes:

$$J_s = \frac{D}{L}\left(2\frac{n_L - n_R}{\delta} - \frac{\alpha - 1}{\alpha\delta}\frac{n_R}{n_0}[n_L e^{(e\Delta V/k_BT)} - n_R]\right)$$

and $J_e = e[(\alpha + 1)J_s - 4D(n_L - n_R)/\delta L)]/(\alpha - 1)$. Using Eq. (5), one deduces an analytical expression for the apparent osmotic pressure in the high surface charge regime:

$$\frac{\Delta\Pi_{\rm app}}{k_BT} = 2\left(1 - \frac{1}{\delta}\right)(n_R - n_L) - \frac{\alpha - 1}{\alpha\delta}\frac{n_R}{n_0}[n_L e^{(e\Delta V/k_BT)} - n_R]. \quad (6)$$

The apparent osmotic pressure, thus, exhibits a rectified salinity gradient contribution coupled to a strong nonlinear dependence on the imposed voltage, with an exponential form that resembles the characteristic equation of a semiconductor diode (Fig. 2). It is interesting to remark that the asymmetry cancels out for $\alpha = 1$, which corresponds to a perfectly asymmetric nanochannel where the two moieties

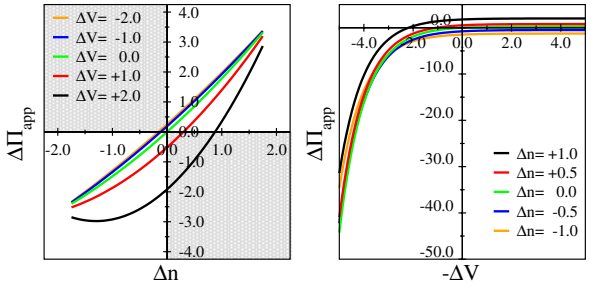

FIG. 2 (color online). Apparent osmotic pressure $\Delta\Pi_{\rm app}$ versus the salinity gradient $\Delta n = n_R - n_L$ (left) and applied voltage $\Delta V = V_R - V_L$ (right) obtained from Eq. (6). Note that the water flux Q, which is the measurable flux, is directly proportional to $\Delta\Pi_{\rm app}$ for vanishing ΔP, see Eq. (3). All the quantities are depicted in reduced units of k_BT, k_BT/e, and n_0 (average salt concentration); $\delta = 3$, $\alpha = 5$.

carry opposite charges ($+\sigma$ and $-\sigma$). Furthermore, note that the apparent divergence of the second term as $\alpha \to 0$ is due to the assumption of a high δ number. Finally, we emphasize here that the predicted exponential dependency of the fluxes with the applied voltage ΔV results from the increasingly large potential gradients inside each part and at junctions inside the channel, and not from an increased salt concentration inside the channel, see the Supplemental Material for details [25]. The previous expression applies for moderate applied voltage, while for very large $e\Delta V/k_BT \gg 1$, the theory predicts that the system goes back into a linear regime with a linear dependence of the fluxes on ΔV associated with surface conduction, see the Supplemental Material [25].

Recalling that in the absence of applied pressure drop $\Delta P = 0$, the flow rate Q is proportional to $\Delta\Pi_{\rm app}$, see Eq. (3), this rectified osmotic pressure directly translates into a rectified water flow. Thus, it behaves as an osmotic diode. To highlight the analogy to Shockley diodes, one may gather formally the various terms in Eq. (6) to write the water flux as

$$Q = \frac{\mathcal{A}}{L}\mathcal{L}_{\rm hyd}\xi k_BT(n_L - n_R) + Q_S[e^{(e\Delta V/k_BT)} - 1], \quad (7)$$

where the expression for the reflection coefficient $\xi(\delta, \alpha, n_L, n_R)$ follows immediately from Eq. (6), and Q_S plays the role of a "limiting water flux" with $Q_S = (\mathcal{A}/L)\mathcal{L}_{\rm hyd} \times k_BTn_Rn_L(1 - \alpha)/(\alpha\delta n_0)$. This phenomenon opens the way toward elaborate control of fluid flows at the nanoscale by coupling salinity and electric gradients. In particular, due to the diodelike dependence of water flux on voltage drop, an oscillating voltage drop is expected to induce a net water flow, which (as quoted above) can be interpreted in terms of rectified electro-osmosis. This is reminiscent of the nanoscale pumping of water by an ac electric field or oscillating charge recently evidenced by molecular dynamics simulations [28,29].

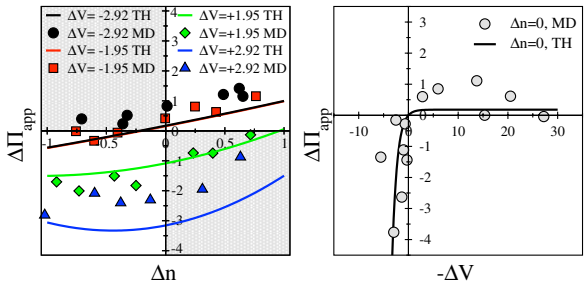

FIG. 3 (color online). Comparison of the theoretical apparent osmotic pressure and the MD simulations results versus the osmotic gradient (left) and the applied voltage (right). As in Fig. 2, the water flux is expected to be proportional to $\Delta\Pi_{\mathrm{app}}$ according to Eq. (3). Surface charges are chosen such that the surface-to-bulk-charge ratios are $\delta_L = 5$ and $\delta_R = \alpha\delta_L$, with $\alpha = 10$. Same units as in Fig. 2.

Molecular dynamics simulations.—In order to assess these counterintuitive behaviors, we present the results of molecular dynamics (MD) simulations of ion and water transport inside a nanochannel using the LAMMPS package [30]. In view of the computational cost required, we have conducted these simulations at two different levels. In a first set of simulations, we focus on the ion dynamics using an implicit solvent. The full ion dynamics is explicitly computed, and the solute flux and electric current are measured, see the Supplemental Material [25]. The osmotic pressure is defined in terms of the solute flux J_s according to Eq. (5). In a second, more detailed level, we performed a restricted number of simulations with full ion + water dynamics to highlight the rectified water flux predicted analytically. In both cases, the geometry is that of Fig. 1. Simulation details are given in the Supplemental Material [25].

Implicit solvent simulations.—Figure 3 (left) presents MD results for the dependence of osmotic pressure with the salinity gradient, under several imposed voltage drops. Despite fluctuations due to thermal noise, a very good agreement with the theoretical predictions of Eq. (6) (solid lines) is found. In particular, the asymmetric behavior can clearly be observed. In Fig. 3 (right), the MD simulations reveal a clear diodelike behavior for the osmotic pressure versus voltage drop, in agreement with the theoretical prediction (solid line). We quote that the voltage values reported here were taken from the direct measurement of the electric potential profiles measured in the system. These are computed using the Coulomb law, taking into account the contributions of all charges in the system and of the external applied field.

Explicit solvent and reverse water flux.—Now, at a level involving full complexity, we present results of MD simulations using water as an explicit solvent. As shown in Fig. 4(a), a system of parallel horizontal graphene slabs is put in contact with two reservoirs. Each side of the horizontal slabs is positively or negatively charged, with a surface charge σ and $-\alpha\sigma$, respectively, creating an array of diodes working in parallel. In the spirit of Ref. [31], air-water interfaces are created at the two ends of the water reservoirs by extending the length of the box in the x direction of the channel, to ensure that the left and right reservoirs are independent and at the same (liquid-vapor coexistence) pressure, although periodic boundary conditions are imposed in all directions.

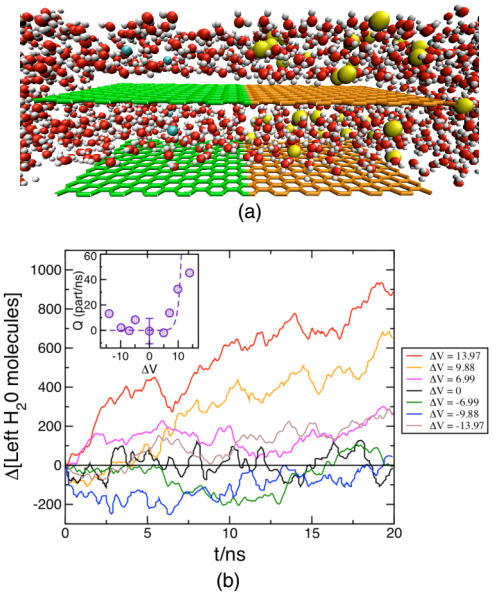

FIG. 4 (color online). (a) View of the simulation system using VMD [33], where parallel graphenelike sheets with asymmetric surface charges act as a membrane. (b) Evolution of the amount of water molecules after 20 ns for various ΔV, with salt concentration $n_R = n_L = 0.15$ M; the surface-to-bulk-charge ratios are $\delta_L = 3$, $\delta_R = 12$. All curves are the average over five realizations of the simulations with duration 20 ns. ΔV is in units of k_BT/e. Inset: Flux $Q = \Delta N_{\mathrm{H_2O}}/\Delta t$ versus the applied voltage drop. The dashed line is an adjustment using the expression $Q = Q_s(\exp[eV/k_BT] - 1)$ with $Q_s = 9 \times 10^{-4}$ ns^{-1}.

This system is obviously much heavier, computationally speaking, than the primitive one; hence, we cannot perform exhaustive measurements with it. However, the expected diodelike water flow is illustrated in Fig. 4(b) for $\Delta n = 0$. We evidence here an asymmetric flow response as a function of the applied voltage: for sufficiently high and positive ΔV, a nonvanishing water flow builds up in the system, while for $\Delta V < 0$, it can hardly be distinguished from the thermal fluctuations (and from the equilibrium situation $\Delta V = 0$). This rectifying behavior of the water flow under voltage drop is in agreement with the theoretical prediction in Eq. (7).

Conclusion.—Altogether, our results demonstrate the possibility of creating an osmotic diode on the basis of asymmetric nanochannels. The osmotic pressure is found to be a nonlinear function of salt concentration difference and voltage drop across the nanochannel, leading to rectified osmotic response. This behavior is similar to the

rectified osmosis observed in various biological systems [17–20]. This also echoes directly the recent experimental report of a rectified electro-osmosis across asymmetric (conical) nanopipettes [32]. Furthermore, our results evidence water flow against the natural osmotic gradient, with water flowing out the high salinity reservoir, depending on the voltage applied. The rectifying character of the diode allows for induced water flow against the osmotic gradient under an oscillating electric field. This opens new perspectives for developing water purification strategies based on voltage-induced reverse osmosis or oscillating electric fields. More generally, the results presented in this Letter open the way toward building true fluidic analogues of nanoelectronic components in order to control fluid flows at the nanoscale.

This research is supported by the ERC Advanced Grant project Micromegas.

*laurent.joly@univ-lyon1.fr
†lbocquet@mit.edu

[1] L. Bocquet and E. Charlaix, Chem. Soc. Rev. **39**, 1073 (2010).
[2] A. Plecis, R. B. Schoch, and P. Renaud, Nano Lett. **5**, 1147 (2005).
[3] I. Vlassiouk and Z. S. Siwy, Nano Lett. **7**, 552 (2007).
[4] X. Hou, W. Guo, and L. Jiang, Chem. Soc. Rev. **40**, 2385 (2011).
[5] Z. Siwy, E. Heins, C. C. Harrell, P. Kohli, and C. R. Martin, J. Am. Chem. Soc. **126**, 10 850 (2004).
[6] Z. Siwy, I. D. Kosinska, A. Fulinski, and C. R. Martin, Phys. Rev. Lett. **94**, 048102 (2005).
[7] H. Daiguji, Y. Oka, and K. Shirono, Nano Lett. **5**, 2274 (2005).
[8] R. Karnik, C. Duan, K. Castelino, H. Daiguji, and A. Majumdar, Nano Lett. **7**, 547 (2007).
[9] O. Kedem and A. Katchalsky, J. Gen. Physiol. **45**, 143 (1961).
[10] M. Elimelech and W. A. Philip, Science **333**, 712 (2011).
[11] B. E. Logan and M. Elimelech, Nature (London) **488**, 313 (2012).
[12] A. Siria, P. Poncharal, A.-L. Biance, R. Fulcrand, X. Blase, S. Purcell, and L. Bocquet, Nature (London) **494**, 455 (2013).
[13] A. V. Raghunathan and N. R. Aluru, Phys. Rev. Lett. **97**, 024501 (2006).
[14] P. J. Atzberger and P. R. Kramer, Phys. Rev. E **75**, 061125 (2007).
[15] A. E. Yaroshchuk, Adv. Colloid Interface Sci. **168**, 278 (2011).
[16] T. W. Lion and R. J. Allen, J. Chem. Phys. **137**, 244911 (2012).
[17] R. E. L. Farmer and R. I. Macey, Biochim. Biophys. Acta **196**, 53 (1970).
[18] C. Toupin, M. L. Maguer, and L. McGann, Cryobiology **26**, 431 (1989).
[19] O. Chara, P. Ford, V. Rivarola, M. Parisi, and C. Capurro, J. Membr. Biol. **207**, 143 (2005).
[20] D. B. Peckys, F. W. Kleinhans, and P. Mazur, PLoS One **6**, e23643 (2011).
[21] G. S. Manning, J. Chem. Phys. **49**, 2668 (1968).
[22] E. V. Dydek, B. Zaltzman, I. Rubinstein, D. S. Deng, A. Mani, and M. Z. Bazant, Phys. Rev. Lett. **107**, 118301 (2011).
[23] D. Constantin and Z. S. Siwy, Phys. Rev. E **76**, 041202 (2007).
[24] I. Vlassiouk, S. Smirnov, and Z. Siwy, ACS Nano **2**, 1589 (2008).
[25] See Supplemental Material at http://link.aps.org/supplemental/10.1103/PhysRevLett.111.244501 for the detailed analytical resolution of the PNP equations under osmotic forcing and voltage drop, as well as for simulation details.
[26] Note that δ resembles the so-called Dukhin number comparing bulk and surface conductances, see Ref. [27].
[27] R. J. Hunter, *Foundations of Colloid Science* (Oxford University, New York, 2001), 2nd ed.
[28] K. F. Rinne, S. Gekle, D. J. Bonthuis, and R. R. Netz, Nano Lett. **12**, 1780 (2012).
[29] J. Kou, X. Zhou, H. Lu, Y. Xu, F. Wu, and J. Fan, Soft Matter **8**, 12 111 (2012).
[30] S. Plimpton, J. Comput. Phys. **117**, 1 (1995); http://lammps.sandia.gov/.
[31] L. Delemotte, F. Dehez, W. Treptow, and M. Tarek, J. Phys. Chem. B **112**, 5547 (2008).
[32] N. Laohakunakorn, B. Gollnick, F. Moreno-Herrero, D. Aarts, R. P. Dullens, S. Ghosal, and U. Keyser, Nano Lett. **13**, 5141 (2013).
[33] W. Humphrey, A. Dalke, and K. Schulten, J. Mol. Graphics **14**, 33 (1996); http://www.ks.uiuc.edu/Research/vmd/.